

PAPER • OPEN ACCESS

Probing exotic neutrino physics with CEvNS

To cite this article: O. G. Miranda *et al* 2021 *J. Phys.: Conf. Ser.* **2156** 012132

View the [article online](#) for updates and enhancements.

You may also like

- [Preliminary test results of LAr prototype detector](#)
Pei-Xian Li, , Meng-Yun Guan et al.
- [Fast component re-emission in Xe-doped liquid argon](#)
D. Akimov, V. Belov, A. Konovalov et al.
- [Design and implementation of the Front End Board for the readout of the ATLAS liquid argon calorimeters](#)
N J Buchanan, L Chen, D M Gingrich et al.



244th ECS Meeting

Gothenburg, Sweden • Oct 8 – 12, 2023

Register and join us in
advancing science!

Learn More & Register Now!



Probing exotic neutrino physics with CEvNS

O. G. Miranda¹, D. K. Papoulias², G. Sanchez Garcia¹, O. Sanders¹,
M. Tórtola³ and J. W. F. Valle³

¹ Departamento de Física, Centro de Investigación y de Estudios Avanzados del IPN, Apartado Postal 14-740 07000 Mexico, Distrito Federal, Mexico

² Division of Theoretical Physics, University of Ioannina, GR 45110 Ioannina, Greece

³ AHEP Group, Institut de Física Corpuscular – CSIC/Universitat de València, Parc Científic de Paterna. C/ Catedrático José Beltrán, 2 E-46980 Paterna (Valencia) - Spain

E-mail: d.papoulias@uoi.gr

Abstract. A new measurement of coherent elastic neutrino-nucleus scattering (CEvNS) on liquid argon (LAr) has been recently reported by the COHERENT experiment. Relying on the new data, we update the status of CEvNS-induced constraints by considering various physics applications, within and beyond the Standard Model. In particular, we explore the implications of the COHERENT-LAr data for electroweak and nuclear physics as well as for interesting scenarios beyond the SM such as NSIs and electromagnetic neutrino properties. We show that compared to the existing constraints derived from the first CEvNS measurement on CsI, the new LAr-dataset yields improved constraints in all cases.

1. Introduction

The COHERENT experiment at the Spallation Neutron Source, after the first observation of coherent elastic neutrino-nucleus scattering (CEvNS) on CsI in 2017 [1], has recently reported a new CEvNS measurement on liquid argon (LAr) [2]. This groundbreaking discovery has opened a new window for exploring various low-energy physics opportunities within and beyond the Standard Model (SM). The most interesting examples in the SM are the determination of the weak mixing angle ($\sin^2 \theta_W$) and the possibility to explore the nuclear rms radius R_n . From the exhaustive list of beyond the SM applications (for a review see Ref. [3]), here we focus on i) nonstandard interactions (NSIs) in the presence of light or heavy new mediators, and ii) electromagnetic neutrino properties such as the effective neutrino magnetic moment and the neutrino charge radius. For the aforementioned cases, in the light of the new LAr data, here we update the existing constraints derived from previous analyses based on CsI data [4, 5].

2. CEvNS within the SM and beyond

The differential CEvNS cross section with respect to the nuclear recoil energy T_A is written as

$$\left(\frac{d\sigma}{dT_A} \right)_{\text{SM}} = \frac{G_F^2 m_A}{2\pi} (Q_W^V)^2 \left[2 - \frac{2T_A}{E_\nu} - \frac{m_A T_A}{E_\nu^2} \right], \quad (1)$$

with E_ν being the incident neutrino energy and Q_W^V denoting the vector weak charge written in the form

$$Q_W^V = (1/2 - 2 \sin^2 \theta_W) Z F_p(Q^2) - 1/2 N F_n(Q^2). \quad (2)$$



Here, the weak mixing angle is taken in the $\overline{\text{MS}}$ scheme, *i.e.* $\sin^2 \theta_W \equiv \hat{s}_Z^2 = 0.2312$, while $F_{p,n}(Q)^2$ denotes the nuclear form factors for protons and neutrons, expressed as

$$F_{p,n}(Q^2) = 3 \frac{j_1(QR_0)}{QR_0} \exp(-Q^2 s^2/2). \quad (3)$$

In the latter expression, the magnitude of the three-momentum transfer is $Q = \sqrt{2m_A T_A}$ and $j_1(x)$ is the first-order spherical Bessel function, while $R_0^2 = \frac{5}{3}(R_{p,n}^2 - 3s^2)$ with $R_n = 3.36$ fm ($R_p = 3.14$ fm) denoting the neutron (proton) rms radius and $s = 0.9$ fm.

Turning our attention to physics beyond the SM, the NSI formalism provides a useful phenomenological description for a large family of new physics models. In this work, we restrict our attention to those leading to modifications of the neutral current SM Lagrangian, parametrized as [6]

$$\mathcal{L}_{NC}^{NSI} = -2\sqrt{2}G_F \sum_{f,P,\alpha,\beta} \varepsilon_{\alpha\beta}^{fP} (\bar{\nu}_\alpha \gamma^\mu P_L \nu_\beta) (\bar{f} \gamma_\mu P_X f), \quad (4)$$

where P_X are the left and right chirality projectors and $\varepsilon_{\alpha\beta}^{fP}$ denote the couplings that quantify the relative strength of the NSI. Specifically, CEvNS is sensitive to NSIs, with $f = \{u, d\}$ being a first-family quark and α, β the neutrino flavors $\{e, \mu, \tau\}$. In the presence of NSIs, the corresponding CEvNS cross section is given from Eq.(1) by substituting the SM weak charge according to $\mathcal{Q}_W^V \rightarrow \mathcal{Q}_{\text{NSI}}^V$ [7]

$$\begin{aligned} \mathcal{Q}_{\text{NSI}}^V &= \left[(g_V^p + 2\varepsilon_{\alpha\alpha}^{uV} + \varepsilon_{\alpha\alpha}^{dV}) ZF_p(Q^2) + (g_V^n + \varepsilon_{\alpha\alpha}^{uV} + 2\varepsilon_{\alpha\alpha}^{dV}) NF_n(Q^2) \right] \\ &+ \sum_{\alpha} \left[(2\varepsilon_{\alpha\beta}^{uV} + \varepsilon_{\alpha\beta}^{dV}) ZF_p(Q^2) + (\varepsilon_{\alpha\beta}^{uV} + 2\varepsilon_{\alpha\beta}^{dV}) NF_n(Q^2) \right]. \end{aligned} \quad (5)$$

As a concrete example, the presence of a sufficiently light vector-mediator (often called the Z') yields NSI-like corrections of the SM cross section through the substitution $\mathcal{Q}_W^V \rightarrow \mathcal{Q}_{Z'}^V$, as [8]

$$\mathcal{Q}_{Z'}^V = \mathcal{Q}_W^V + \frac{g_{Z'}^{\nu V}}{\sqrt{2}G_F} \frac{(2g_{Z'}^{uV} + g_{Z'}^{dV}) ZF_p(Q^2) + (g_{Z'}^{uV} + 2g_{Z'}^{dV}) NF_n(Q^2)}{2m_A T_A + M_{Z'}^2}. \quad (6)$$

At this point, it is worth noting that the latter expression for the case of a heavy mediator reduces to the usual NSI weak charge given Eq.(5)

On the other hand, assuming a scalar boson mediating the CEvNS process, due to the absence of interference with the SM, the total cross section is given by $(d\sigma/dT_A)_{\text{tot}} = (d\sigma/dT_A)_{\text{SM}} + (d\sigma/dT_A)_{\text{scalar}}$. The purely scalar contribution in this case, is given by [8]

$$\left(\frac{d\sigma}{dT_A} \right)_{\text{scalar}} = \frac{G_F^2 m_A^2}{4\pi} \frac{g_\phi^{qS} Q_\phi^2 T_A}{E_\nu^2 (2m_A T_A + M_\phi^2)^2}, \quad (7)$$

where the corresponding scalar charge takes the form [9]

$$\mathcal{Q}_\phi = ZF_p(Q^2) \sum_{q=u,d} g_\phi^{qS} \frac{m_p}{m_q} f_{T_q}^p + NF_n(Q^2) \sum_{q=u,d} g_\phi^{qS} \frac{m_n}{m_q} f_{T_q}^n, \quad (8)$$

while the hadronic form factors $f_{T_q}^q$, are taken from Ref. [10].

Finally, non-trivial electromagnetic (EM) neutrino interactions are also plausible in view of the massive neutrinos implied by the discovery of neutrino oscillations. The two main

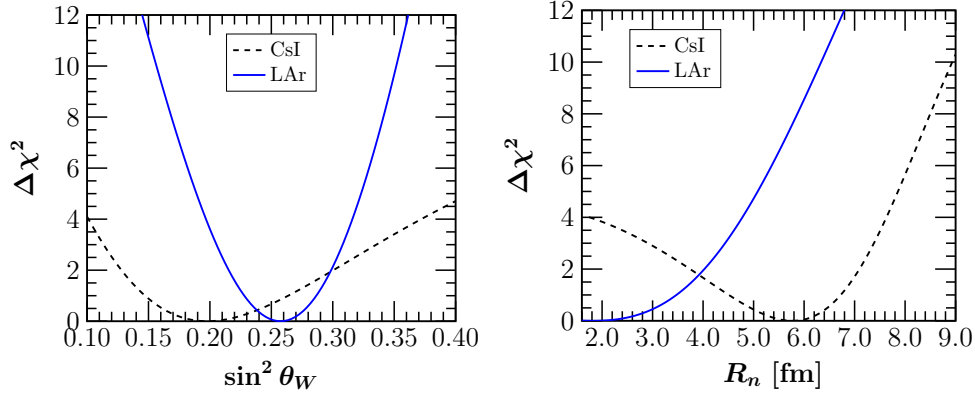


Figure 1. Sensitivity on the weak mixing angle (left) and on the neutron rms radius (right). Figure taken from Ref. [12].

phenomenological EM neutrino parameters that CEvNS is sensitive to, are the effective neutrino magnetic moment μ_{ν_α} and the neutrino charge radius $\langle r_{\nu_\alpha}^2 \rangle$. The former, flips the helicity and therefore leads to a new EM-induced contribution that adds incoherently to the CEvNS cross section and is given by [11]

$$\left(\frac{d\sigma}{dT_A} \right)_{\text{EM}} = \frac{\pi a_{\text{EM}}^2 \mu_\nu^2 Z^2}{m_e^2} \left(\frac{1 - T_A/E_\nu}{T_A} \right) F_p^2(Q^2). \quad (9)$$

On the other hand, the neutrino charge radius is a helicity-preserving quantity that is taken into account through a redefinition of the weak mixing angle as:

$$\sin^2 \theta_W \rightarrow \hat{s}_Z^2 + \frac{\sqrt{2}\pi\alpha_{\text{EM}}}{3G_F} \langle r_{\nu_\alpha}^2 \rangle \quad (10)$$

with α_{EM} being the fine structure constant.

3. Results and discussion

In this section we summarize the main results obtained Ref. [12] in the light of the new COHERENT-LAr data. In all cases (see below), the new LAr-driven analysis indicates improved constraints compared to those extracted from the respective CsI-driven analysis.

Focusing first on the SM interactions only, in Fig. 1 we present the χ^2 sensitivity profiles of the weak mixing angle (left) and the nuclear neutron rms radius (right). For the weak mixing angle our fit indicates the following limits at 90% C.L.

$$\sin^2 \theta_W = 0.258_{-0.050}^{+0.048} \text{ (LAr)} \quad \text{and} \quad \sin^2 \theta_W = 0.197_{-0.080}^{+0.124} \text{ (CsI)}. \quad (11)$$

Similarly, for the case of the nuclear neutron rms radius we find at 90% C.L.

$$R_n < 4.33 \text{ fm (LAr)} \quad \text{and} \quad R_n = 5.6_{-2.1}^{+1.5} \text{ fm (CsI)}. \quad (12)$$

We need to stress, however, that in the latter case the two results are not comparable since they refer to different nuclear isotopes. In addition, it is interesting to notice that the LAr data imply only an upper bound while the CsI data lead to a constrained region.

Turning to NSIs and by assuming one non-vanishing coupling at a time, in Fig. 2 we illustrate the obtained sensitivity on the flavor-changing $\epsilon_{\alpha\beta}^{dV}$ parameters (left panel) and nonuniversal

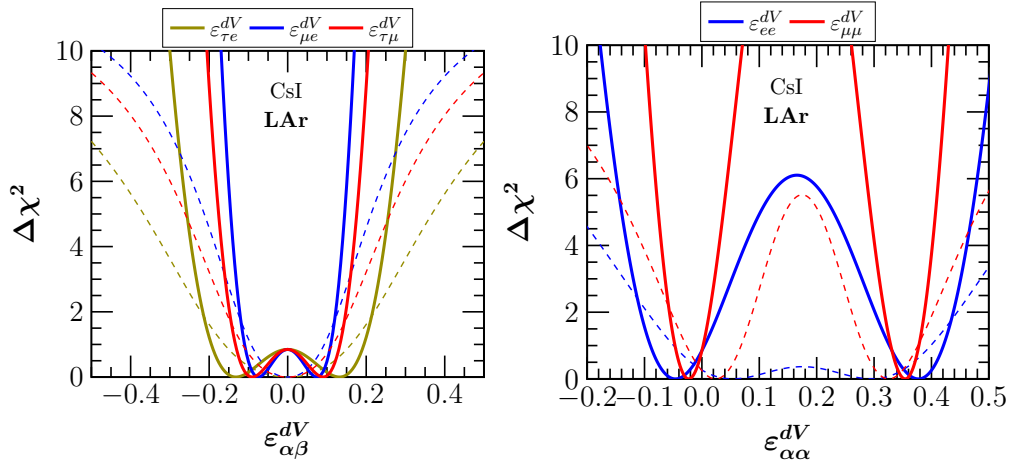


Figure 2. Sensitivity on the flavor changing (left) and non-universal (right) NSI couplings. Figure taken from Ref. [12].

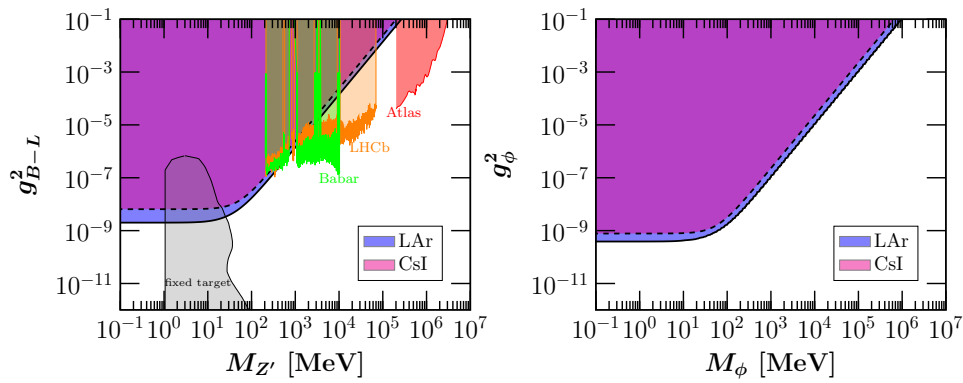


Figure 3. Excluded region at 90% C.L in the parameter space ($M_{Z'}, g_{B-L}^2$) for the vector mediator scenario (left) and (M_ϕ, g_ϕ^2) for the scalar mediator scenario (right). Figure taken from Ref. [12].

$\epsilon_{\alpha\alpha}^{dV}$ parameters (right panel). Evidently, in all cases the LAr data (solid lines) lead to more stringent constraints compared to those obtained from the CsI data (dashed lines). We now consider potential contributions to CEvNS by the vector-mediator associated to the $U(1)_{B-L}$ extension of the SM, *i.e.* by imposing $g_{Z'}^{qV} = -g_{Z'}^{\nu V}/3$. The left panel of Fig. 3 shows the allowed regions in the $(M_{Z'}, g_{B-L}^2)$ parameter space. As can be seen from the plot, CEvNS data offer complementary constraints to those extracted from fixed target experiments in the low-energy regime ($1 \leq M_{Z'} \leq 100$ MeV) as well as to the corresponding ones from the analysis of Babar, LHCb and ATLAS data for the case of heavy mediators *e.g.* for $M_{Z'} > 1$ GeV. Moreover, the right panel of Fig. 3 shows the corresponding allowed regions in the (M_ϕ, g_ϕ^2) plane for the case of a scalar mediator.

Finally, in Fig. 4 we present the extracted constraints on the effective neutrino magnetic moment (left panel) and charge radius (right panel). For the neutrino magnetic moment, the obtained constraints from the analysis of the COHERENT-LAr data at 90% C.L. read [12]

$$(\mu_{\nu_e}, \mu_{\nu_\mu}, \mu_{\bar{\nu}_\mu}) < (94, 53, 78) 10^{-10} \mu_B, \quad (13)$$

and imply only a slight improvement with respect to the CsI data. For case of the neutrino

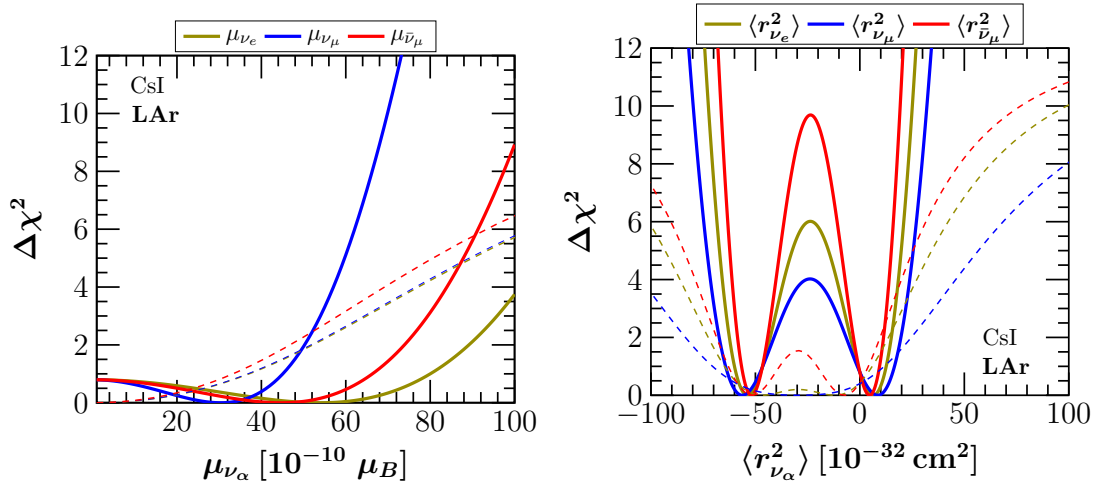


Figure 4. Sensitivity to the neutrino magnetic moment (left) and charge radius (right). Figure taken from Ref. [12].

charge radius the constraints at 90% C.L. read [12]

$$\begin{aligned}
 \langle r_{\nu_e}^2 \rangle &= (-64, -41) \text{ and } (-7, 16), \\
 \langle r_{\nu_\mu}^2 \rangle &= (-69, -37) \text{ and } (-10, 21), \\
 \langle r_{\bar{\nu}_\mu}^2 \rangle &= (-60, -43) \text{ and } (-5, 12),
 \end{aligned} \tag{14}$$

in units of 10^{-32} cm^2 . For the latter case, unlike the neutrino magnetic moment, a significant improvement compared to the first CsI-analysis is found.

4. Acknowledgments

Work supported by the Spanish grants PID2020-113775GB-I00 (AEI / 10.13039/501100011033) and PROMETEO/2018/165 (Generalitat Valenciana) and by CONACYT-Mexico under grant A1-S-23238. O. G. M. has been supported by SNI (Sistema Nacional de Investigadores). The work of DKP is co-financed by Greece and the European Union (European Social Fund-ESF) through the Operational Programme ‘‘Human Resources Development, Education and Lifelong Learning’’ in the context of the project ‘‘Reinforcement of Postdoctoral Researchers - 2nd Cycle’’ (MIS-5033021), implemented by the State Scholarships Foundation (IKY).

References

- [1] Akimov D *et al.* (COHERENT) 2017 *Science* **357** 1123–1126 (*Preprint* 1708.01294)
- [2] Akimov D *et al.* (COHERENT) 2021 *Phys. Rev. Lett.* **126** 012002 (*Preprint* 2003.10630)
- [3] Papoulias D K, Kosmas T S and Kuno Y 2019 *Front. in Phys.* **7** 191 (*Preprint* 1911.00916)
- [4] Papoulias D K and Kosmas T S 2018 *Phys. Rev. D* **97** 033003 (*Preprint* 1711.09773)
- [5] Papoulias D K 2020 *Phys. Rev. D* **102** 113004 (*Preprint* 1907.11644)
- [6] Miranda O G and Nunokawa H 2015 *New J. Phys.* **17** 095002 (*Preprint* 1505.06254)
- [7] Barranco J, Miranda O G and Rashba T I 2005 *JHEP* **12** 021 (*Preprint* hep-ph/0508299)
- [8] Cerdeño D G, Fairbairn M, Jubb T, Machado P A N, Vincent A C and Boehm C 2016 *JHEP* **05** 118 [Erratum: *JHEP* 09, 048 (2016)] (*Preprint* 1604.01025)
- [9] Aristizabal Sierra D, Dutta B, Liao S and Strigari L E 2019 *JHEP* **12** 124 (*Preprint* 1910.12437)
- [10] Hoferichter M, Ruiz de Elvira J, Kubis B and Meißner U G 2015 *Phys. Rev. Lett.* **115** 092301 (*Preprint* 1506.04142)
- [11] Vogel P and Engel J 1989 *Phys. Rev. D* **39** 3378
- [12] Miranda O G, Papoulias D K, Sanchez Garcia G, Sanders O, Tórtola M and Valle J W F 2020 *JHEP* **05** 130 [Erratum: *JHEP* 01, 067 (2021)] (*Preprint* 2003.12050)